Magnetic Resonance Imaging, Vol. 16, No. 9, pp. 1057–1073, 1998

Printed in the USA.
0730-725X/98 $19.00 + .00

PII S00730-725X(98)00130-1

● *Original Contribution*

TEMPORAL SAMPLING REQUIREMENTS FOR THE TRACER KINETICS MODELING OF BREAST DISEASE

ELIZABETH HENDERSON,* BRIAN K. RUTT,*† AND TING-YIM LEE*†‡

*Lawson Family Imaging Research Laboratories, Robarts Research Institute, London, Ontario; †Department of Diagnostic Radiology, London Health Sciences Centre, University Campus, London, Ontario; and ‡Department of Radiology and Lawson Research Institute, St. Joseph's Health Centre, London, Ontario, Canada

The physiological parameters measured in the tracer kinetics modeling of data from a dynamic contrast-enhanced magnetic resonance (MR) breast exam (blood flow-extraction fraction product [FE], volume of the extracellular extravascular space [V_e], and blood volume [V_b]) may enable non-invasive diagnosis of breast cancer. One of the factors that compromises the accuracy and precision of the parameter estimates, and therefore their diagnostic potential, is the temporal resolution of the MR scans used to measure contrast agent (gadolinium-diethylenetriamine pentaacetic acid [Gd-DTPA]) concentration in an artery (arterial input function [AIF]) and in the tissue (tissue residue function [TRF]). Using computer simulations, we have examined, for several AIF widths, the errors introduced into estimates of tracer kinetic parameters in breast tissue due to insufficient temporal sampling. Temporal sampling errors can be viewed as uncertainties and biases in the parameter estimates introduced by the uncertainty in the relative alignments of the AIF, TRF, and sampling grid. These effects arise from the model's inherent sensitivity to error in either the AIF or TRF, which is dependent on the values of the tracer kinetic parameters and increases with AIF width. Based on the results of the simulations, to ensure that the error in FE and V_e will be under 10% of their true values, we recommend a rapid bolus injection of contrast agent (~10 s), that the AIF be sampled every second, and that the TRF be sampled every 16 s or less. An accurate measurement of V_b requires that the TRF be sampled at least every 4 s. The results of these investigations can be used to set minimum dynamic imaging rates for tracer kinetics modeling of the breast.

Keywords: **Temporal sampling; Tracer kinetics model; Breast; Contrast agent.**

INTRODUCTION

Dynamic contrast-enhanced magnetic resonance imaging (MRI) has potential for achieving good specificity in breast cancer diagnosis. The enhancement versus time curves of benign and malignant lesions tend to have distinctive shapes. After a rapid bolus injection of a contrast agent, most malignant lesions enhance rapidly and plateau within a few minutes whereas benign tumours generally enhance at a much slower rate.[1–5] Because of this observation, many authors have used enhancement indices, such as the maximum tissue enhancement, the tissue enhancement at various time points, and the initial rate of contrast agent uptake, as a basis for differentiating between benign and malignant breast lesions.[1,4–10] Attempts at breast cancer diagnosis using enhancement indices, however, have not yielded consistent results. Specificity measurements based on enhancement indices vary between 65% and 100%.[1,4–11] Furthermore, some have suggested that enhancement indices alone are not sufficient for differentiating between benign and malignant tissue.[10,12–14]

On the other hand, the moderate success achieved in these studies, and other work on tumour angiogenesis,[15,16] suggests that there may be physiological differences between breast abnormalities that are responsible for the distinctive appearances of the contrast agent uptake curves of benign and malignant tissues. In addition, measurements of parameters, expressed in tissue contrast agent uptake curves, which relate to tumour angiogenesis,

RECEIVED 10/10/97; ACCEPTED 4/15/98.

Address correspondence to Ting-Yim Lee, Lawson Family Imaging Research Laboratories, Robarts Research Institute, P.O. Box 5015, 100 Perth Drive, London, Ontario, Canada, N6A 5K8. E-mail: tlee@irus.rri.on.ca

may have a role in assessing patient prognosis or treatment planning. For example, the steepest slope of contrast enhancement in tumours has been correlated with microvessel density,[10] an indicator of the degree of tissue angiogenesis and an independent prognostic indicator for the metastatic potential of a tumour.[17,18] A direct, accurate measurement of parameters that fundamentally describe the tissue vasculature may enable improved specificity in breast cancer diagnosis, and could have a role in the staging of breast cancer patients.

Due to the above considerations, there has recently been a trend toward applying a tracer kinetics model to dynamic contrast-enhanced MRI data in order to extract parameters that reflect the state of the tissue vasculature, and hence the degree of angiogenesis.[19–25] To obtain quantitative vascular parameters from a tracer kinetics model, a measurement must be made of the time course of contrast agent in the tissue of interest (tissue residue function [TRF]) and, in addition, the time course of contrast agent in an artery (arterial input function [AIF]) must either be measured or assumed. When the tracer kinetics model is fit to these two time courses, parameters such as the flow-extraction fraction product (FE), the capillary permeability surface area product (PS), the volume of the extracellular, extravascular space (V_e), and the blood volume (V_b) can be estimated. Hulka et al.[22] have demonstrated the improved specificity attained with FE estimates compared to that achieved using an enhancement index. In addition, van Dijke et al.[26] showed, in an animal breast cancer model, that plasma volume and microvascular permeability are significantly correlated with microvessel density. Tracer kinetic parameters do appear to be indicative of tumour angiogenesis and, if indeed there are fundamental differences between benign and malignant tumours, then it is likely that more accurate measurements of tracer kinetic parameters will enable improved separation between the two groups.

However, one of the inherent limitations of dynamic contrast-enhanced MRI, and especially of multislice or three-dimensional (3D) dynamic imaging, is its generally low temporal resolution. Insufficient temporal sampling of the TRF and the AIF will certainly have an effect on the accuracy of tracer kinetic parameter estimates, and can therefore be expected to reduce the potential specificity of the parameters. Although a number of studies have examined the effects of insufficient temporal resolution under certain conditions,[11,20,27] there are currently no accepted guidelines on the temporal resolution required for accurate parameter estimates. Whereas most studies attempt to maximize the temporal sampling rate, different tracer kinetics modeling studies have employed widely different temporal sampling rates. Comparisons between the results of different studies are therefore difficult. Furthermore, in practice, improvements in temporal resolution usually necessitate a sacrifice in spatial resolution. Knowledge of the errors introduced into the estimates of tracer kinetic parameters by insufficient temporal sampling would enable a better understanding of the quantitative accuracy of previous measurements, and an optimization of both temporal and spatial resolutions for future studies.

The purpose of this work was to investigate, using computer simulations, the effect of finite temporal sampling of the AIF and the TRF on the accuracy with which tracer kinetic parameters (FE, V_b, and V_e) may be estimated and thereby to provide recommendations for the setting of dynamic imaging rates in future studies. An earlier version of this work has been presented previously.[28] We introduce the concept of temporal jitter uncertainty, which is an uncertainty introduced into the kinetic parameter estimates as a result of the uncertainty in the relative alignments of the AIF, the TRF, and the sampling grid (array of imaging times). We also examine the model's inherent sensitivity to error in the TRF measurement using covariance (COV) matrices. Variations in error due to temporal sampling are examined as a function of the values of the kinetic parameters and width of the AIF for two possible experimental situations: that in which the AIF and the TRF are sampled at the same rate and that in which the AIF is sampled much more frequently than the TRF. The latter strategy will likely prove to be more practical for imaging studies, as it allows the temporal sampling constraints for the TRF to be relaxed significantly. We conclude that, for accurate (less than 10% relative error) estimates of FE and V_e only, the TRF should be sampled at least every 16 s, whereas the AIF should be sampled every second or less. For an accurate measurement of V_b, the sampling constraint for the TRF must be increased to at least once every 4 s. In addition, the contrast agent should be administered as a rapid bolus. These recommendations will be useful for setting the dynamic imaging rates for future tracer kinetics modeling studies of the breast.

THEORY

Tracer Kinetics Model

The time course of contrast agent concentration in a volume of breast tissue ($C_t(t)$ [mmol/g]) is described by the following equation:[29,30]

$$C_t(t) = FE\, C_a(t - t_0) \otimes e^{-\frac{FE}{V_e}(t - t_0)} + V_b C_a(t - t_0) \qquad (1)$$

where $\otimes$ indicates a convolution operation, t_0 [min] is the time separating the arrival of contrast agent in the artery from its arrival in the tissue and $C_a(t)$ [mmol/mL] is the arterial concentration of contrast agent. V_e [mL/g] and

V_b [mL/g] are the distribution volumes of the contrast agent within the extravascular extracellular and blood compartments respectively, and FE [mL/min/g] is the product of blood flow (F [mL/min/g]) and the extraction fraction (E) of the contrast agent (gadolinium–diethylenetriamine pentaacetic acid [Gd-DTPA]). We chose to use this tracer kinetics model as it takes into account the fact that the permeability-surface area product (PS) of Gd-DTPA in breast tissue is on the order of blood flow, and because the parameters that this model estimates relate directly to the tissue vasculature. This model is mathematically identical to the general form of the Tofts and Kermode model,[31,32] and the temporal sampling requirements for $C_a(t)$ and $C_t(t)$ are independent of the interpretation of the kinetics parameters. $C_a(t)$ and $C_t(t)$ are also referred to as the AIF and the TRF, respectively.

In dynamic contrast-enhanced magnetic resonance imaging (MRI) studies, $C_t(t)$ can be calculated from the change in image intensity following a bolus injection of Gd-DTPA, assuming appropriate calibration is performed.[31,33–35] Determining $C_a(t)$ is somewhat more difficult. If a large artery can be included in the image field of view, then $C_a(t)$ can also be calculated from the changing image intensity of the artery in the dynamic series, although difficulties arising from factors such as flow effects and oblique vessels must be overcome. $C_a(t)$ can also be determined by arterial blood sampling[33,34] or by assuming a general shape.[21] Because the temporal sampling rates for the TRF and often for the AIF are finite, parameter accuracy will suffer. The temporal sampling issue is of particular concern for 3D dynamic imaging of the breast.

Temporal Jitter

A complication to studies of the effect of insufficient temporal sampling of the AIF and TRF on estimates of tracer kinetic parameters is the phenomenon of temporal jitter. In practice, it is impossible to synchronize the sampling grid, which is the array of time points at which the TRF or AIF are sampled, with the arrival of contrast agent at the artery or tissue (Fig. 1). Even if the first sample is always taken at the beginning of the initial rise of the AIF, variations in the transit time between the artery and the tissue and in cardiac output mean that the delay between the AIF and the TRF, (ϵ–δ as defined in Fig. 1), will always be unknown. The uncertainty in the relative temporal positions of the AIF, TRF, and the sampling grid can have a large effect on the accuracy with which the parameters can be determined, as we will show in this paper, but is unpredictable in an experimental situation.

Sensitivity Functions and COV Matrix Calculations

The precision with which a model is able to measure tracer kinetic parameters can be examined qualitatively using sensitivity functions (Fig. 2) and quantitatively by calculating COV matrices.[36] Sensitivity functions, $SF_i(t)$, of the tracer kinetic parameters are defined as:

$$SF_i(t) = \frac{\partial C_t(t)}{\partial p_i},\ i = 1, 2, \ldots n \qquad (2)$$

where p_i is the i^{th} tracer kinetic parameter (in this case, $n = 3$). Therefore, if the i^{th} parameter, p_i, is changed by Δp_i, then $C_t(t)$ will change by $\Delta p_i \cdot SF_i(t)$. The magnitude of a sensitivity function over the time course of the experiment is an indication of the suitability of the model for estimations of that particular parameter. The more similar two sensitivity functions are, the less a fitting routine is able to distinguish between the two corresponding parameters.

A COV matrix can be calculated from the sensitivity functions:[37]

$$COV = \sigma^2(F^TF)^{-1},\ F_{ij} = SF_i(j) \qquad (3)$$

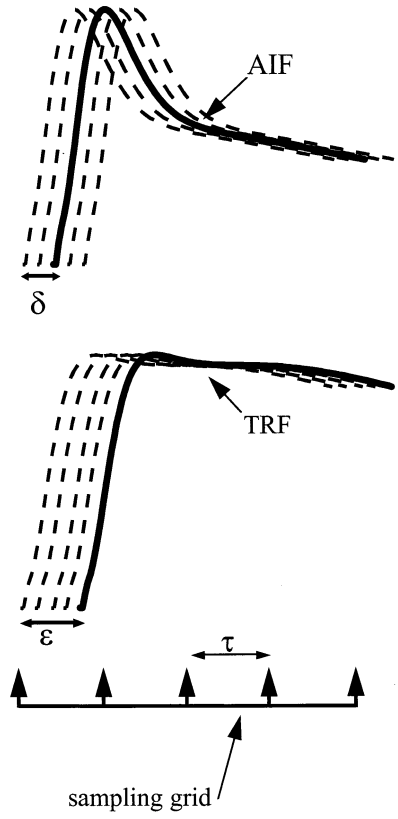

Fig. 1. The AIF and TRF are both sampled at a rate τ, and are offset from the start of the sampling interval by times δ and ϵ, respectively. In an experimental situation, δ and ϵ are unknown, and the uncertainty in these two parameters will therefore introduce an uncertainty in the estimates of the kinetic parameters.

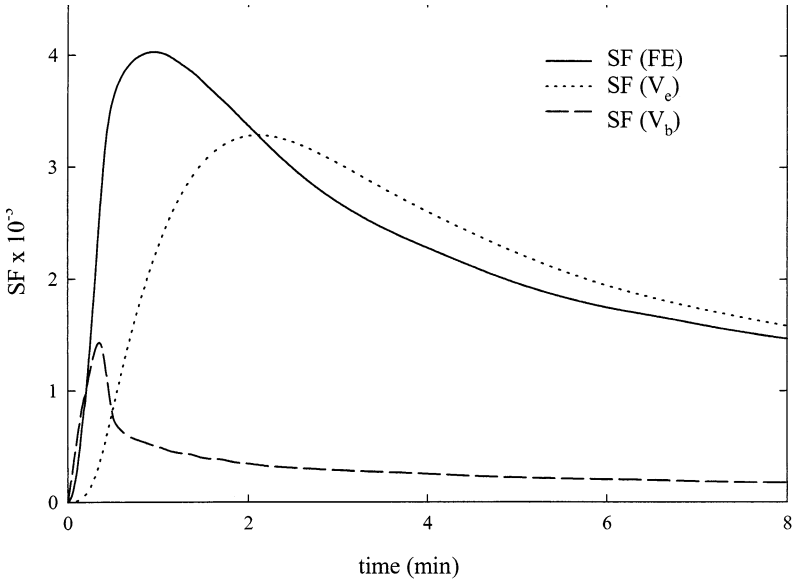

Fig. 2. Sensitivity functions for the tracer kinetics model represented by Eq. (1) with FE = 0.5 mL/min/g, V_e = 0.4 mL/g, V_b = 0.05 mL/g, and an AIF corresponding to a 10-s bolus injection of Gd-DTPA (1 × AIF).

where σ^2 is the noise variance in the TRF. The diagonal elements of the COV matrix are the variances of the parameter estimates, and each represents the expected uncertainty in the estimate of the corresponding parameter due to noise in the TRF measurement. The off-diagonal elements are the COV of the parameters and indicate how errors in estimates of the parameters interact. For example, if the COV between two parameters is negative, then if one parameter is overestimated, the other will tend to be underestimated, assuming no bias in the parameter estimates. COV matrices are therefore a useful tool for predicting how the error in each parameter will vary with parameter value or AIF width.

Insufficient temporal sampling of the TRF means that high frequency information is lost. This loss, when considered together with the effect of temporal jitter, manifests itself as an uncertainty in the TRF measurement. We therefore investigated the use of COV matrices for predicting trends in errors arising from uncertainties in the TRF introduced by temporal jitter, rather than noise. Because we are examining the relative effects of different temporal sampling rates, then, without the loss of generality, we will set the noise variance (σ^2) of the TRF to be equal to one.

MATERIALS AND METHODS

The effect of temporal sampling on the accuracy of tracer kinetic parameter estimates was examined through a series of computer simulations. The error introduced by insufficient temporal sampling is highly dependent on the shapes of both the arterial input function and the tissue residue function. Therefore, the simulations were repeated for many sets of values of the kinetic parameters (FE, V_e, V_b) as well as for several widths of the arterial input function. The trends found in the computer simulations were compared with the predictions of the COV matrices. In addition, two different sampling strategies were studied.

The arterial input function used in the simulations was a published curve[38] obtained by withdrawing arterial blood samples every 10 s following a 10-s bolus injection of Gd-DTPA. We digitized this curve and then interpolated it by cubic Hermite polynomials to 0.25-s temporal resolution, using the NAG Fortran library routines E01BEF and E01BFF (The Numerical Algorithms Group Ltd., Downers Grove, IL).[39] Note that because the original AIF was measured at 10-s intervals, the high frequency components in the peak of the curve that may be present in a true AIF are not represented in the AIF used in the simulations. In order to simulate the effect of a slower injection rate, the original interpolated curve was stretched in the time direction by factors of 2, 4, and 8 (Fig. 3). The area under the AIF was conserved to simulate a constant injected dose. Although the stretching operation does not exactly reproduce the combined effects of the injection duration and the underlying physiology, these curves roughly correspond to the AIFs that would be observed following a 40-s, 80-s, and 160-s injection of contrast agent, respectively. Both the TRF and the AIF had a total length of 8 min.

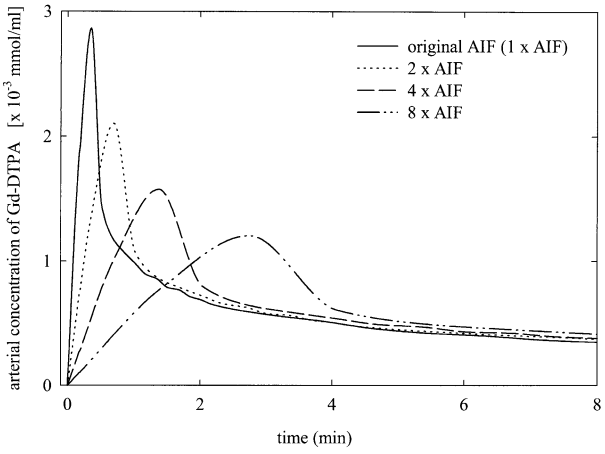

Fig. 3. The four AIFs used in the computer simulations. The width of the AIF was varied by stretching an AIF (digitized from Andersen et al.[38]), corresponding to a 10-s bolus injection of Gd-DTPA (1 × AIF), in the time direction by factors of 2 (2 × AIF), 4 (4 × AIF), and 8 (8 × AIF).

The literature was surveyed to determine the anticipated range of values for the tracer kinetic parameters in breast tumour tissue (Table 1). Based on the reported values of FE, V_e, and V_b, we considered FE values ranging between 0.1 and 1.3 mL/min/g, V_e values ranging between 0.1 and 0.8 mL/g, and V_b values ranging between 0.01 and 0.125 mL/g.

High temporal resolution TRFs were generated from the AIFs using the tracer kinetics model equation (Eq. 1). Many sets of parameter values were studied. Because investigating every possible combination of values of the tracer kinetic parameters is impossible, each parameter was varied in turn, while the other two parameters were held constant at a mean value. The mean values used for FE, V_e, and V_b were 0.5 mL/min/g, 0.4 mL/g, and 0.05 mL/g, respectively. In this way, the trends in the errors arising from temporal sampling could be evaluated as a function of parameter value. Tissue residue functions generated for several sets of parameter values (FE, V_e, and V_b) are shown in Fig. 4.

Table 1. Values of tracer kinetic parameters in breast tumours reported in the literature

Reference	FE (mL/min/g)	V_e (mL/g)	V_b (mL/g)*
(21)†	0.1–1.3	0.3–0.8	—
(22)-cancers	0.45 ± 0.22	—	—
(22)-benign	0.17 ± 0.11	—	—
(24)†-cancers	2.04 ± 1.20	0.45 ± 0.18	0.26 ± 0.12
(24)†-benign	0.90 ± 0.78	0.47 ± 0.19	0.17 ± 0.10
(26)‡	—	—	0.0–0.26
(40)‡	—	—	0.047 ± 0.02

* Plasma volume.
† Assuming that tissue density is 1.0 mL/g.
‡ Human mammary carcinoma in the mammary fat pads of athymic rats.

There are two basic strategies that could be employed for carrying out quantitative dynamic contrast-enhanced MR exams. In one, an artery is included in the same image slice as the tissue of interest, and therefore both the AIF and the TRF are sampled simultaneously at every image time (time of centre of k-space acquisition). In the other possible strategy, the AIF is sampled at a much finer temporal resolution than the TRF, either by an interleaving strategy such as that proposed by Taylor et al.[41] or by using a general, assumed AIF, which is known at high temporal resolution.[21] Preliminary investigations[28] showed that in the second sampling strategy, the requirements for sampling of the TRF would be relaxed significantly compared to the first strategy. Therefore, in one set of simulations, both the AIF and the TRF were sampled by digitally picking points every 1 s, 2 s, 4 s, 6 s, 8 s, . . . , and 20 s. In the second set of simulations, the interval at which the AIF was sampled was held constant at 1 s, while the TRF was sampled every 4 s, 8 s, 12 s, 16 s, . . . , and 44 s. This sampling methodology simulates the idealized case in which all of k-space is collected instantaneously.

Prior to sampling, the AIF and TRF were shifted by various fractions of the sampling interval (δ/τ and ϵ/τ, respectively [Fig. 1]) in order to simulate the effect of temporal jitter. For the first sampling situation, in which both curves are sampled at the same rate, both the AIF and TRF were shifted by 0, 1/4, 1/2, and 3/4 of the sampling interval, τ, making 16 combinations. In the second sampling simulation, in which the temporal resolution of the AIF is much higher than that of the TRF, only the TRF was shifted by multiples of 1/16th of the sampling interval, again making 16 combinations.

Parameter estimates were calculated using the quasi-Newton bounded minimization routine E04JAF from the NAG Fortran Library.[39] As a pre-processing step, the sampled AIFs input to this program were interpolated via a cubic Hermite polynomial interpolation to 0.5-s intervals in order to improve upon the accuracy in the evaluation of the convolution integral in Eq. (1). Four parameters were solved for: FE, V_e, V_b, and t_o, the time difference between the beginning of the AIF and the beginning of the TRF. FE, V_e, and V_b were all constrained to be non-negative. Finally, in order to test that the fitting routine had converged to a global minimum, three different sets of initial parameter values were supplied to the fitting program, and, if more than one solution was found, indicating fit instability, the set of parameter values that minimized the sum of squared residuals was accepted. For each TRF, AIF, sampling

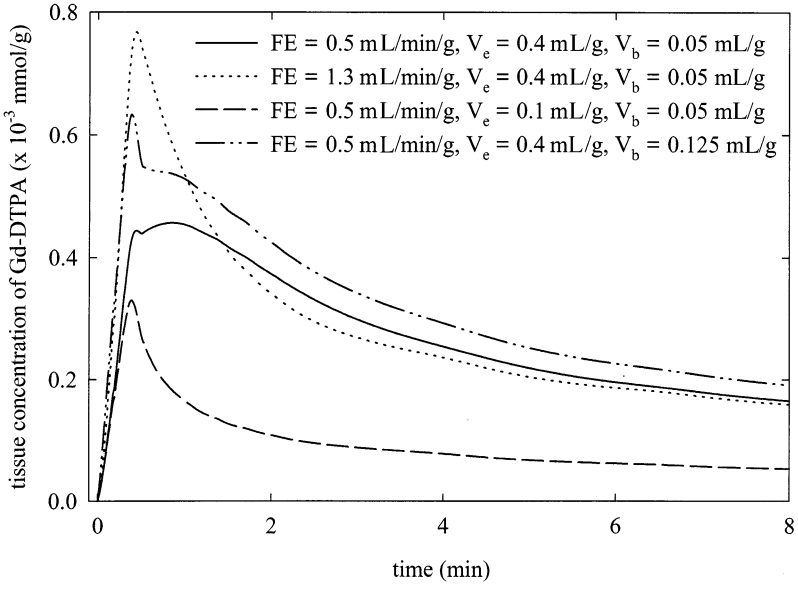

Fig. 4. TRF for several different sets of values for the tracer kinetic parameters FE, V_e, and V_b. All curves were generated using the narrowest AIF (1 × AIF).

rate, and sampling strategy, 16 sets of parameter estimates were calculated, from the 16 possible combinations of AIF and TRF shifts.

RESULTS

Effect of Temporal Sampling

Temporal jitter introduces an uncertainty into the parameter measurements (Fig. 5). Therefore, the effect of temporal sampling on the parameter estimates can be expressed as a bias (B) in the mean of the 16 temporal jitter parameter estimates and as an uncertainty or standard deviation (ΔB). If we assume that the uncertainty in the parameter estimates introduced by temporal jitter follows a Gaussian distribution, then a 95% confidence interval (B ± 1.96 ΔB) for the parameter estimates can be calculated (Fig. 5b). The bias and uncertainty are a function of the sampling interval, the width of the AIF, and the values of the tracer kinetic parameters (FE, V_e, and V_b). The uncertainty always increases with increasing sampling interval. By sampling the AIF every second, the effect of temporal jitter can be significantly decreased (Fig. 5c) compared to sampling both the AIF and TRF at the same rate.

For sampling intervals of 20 s and above, the fitting routine does not always converge to a global minimum due to the small number of data points. In these cases, temporal sampling errors arise from two sources: temporal jitter and fit instability, and increase rapidly with increasing sampling interval. Unfortunately, as long as experiment time is limited, fit instability is unavoidable for low sampling frequencies.

Predictions of the COV Matrices

The COV matrices predict an increase in the uncertainty in the parameter estimates, due to noise or temporal jitter, as a function of AIF width. Also, the matrices predict that uncertainties in all three parameters will increase as a function of FE and decrease with increasing V_e. The uncertainties in the estimates of FE and V_e are independent of the value of V_b, but the uncertainty in V_b decreases as V_b is increased. For example, Fig. 6 demonstrates how the variance of the FE estimate increases as a function of FE and width of the AIF, as predicted by COV matrix calculations. The COV matrices successfully predict the trends in ΔB seen with AIF width and tracer kinetic parameter value described below.

Effect of AIF Width

When both the AIF and the TRF are sampled every second, increasing the width of the AIF increases the bias in all mean parameter estimates (Fig. 7, τ = 1 s). This effect is most pronounced for large values of FE (Fig. 7c) or for small values of V_e or V_b. This trend with AIF width disappears when both the AIF and TRF are sampled at higher sampling intervals (Fig. 7, τ = 16 s). In this case, both B and ΔB become large, particularly for the narrowest AIF (1 × AIF).

If the AIF is sampled at a much higher frequency (i.e., every second) compared to the TRF, both B and ΔB are reduced substantially (Fig. 8). In general, as the width of the AIF is reduced, both B and ΔB become less sensitive to increasing τ.

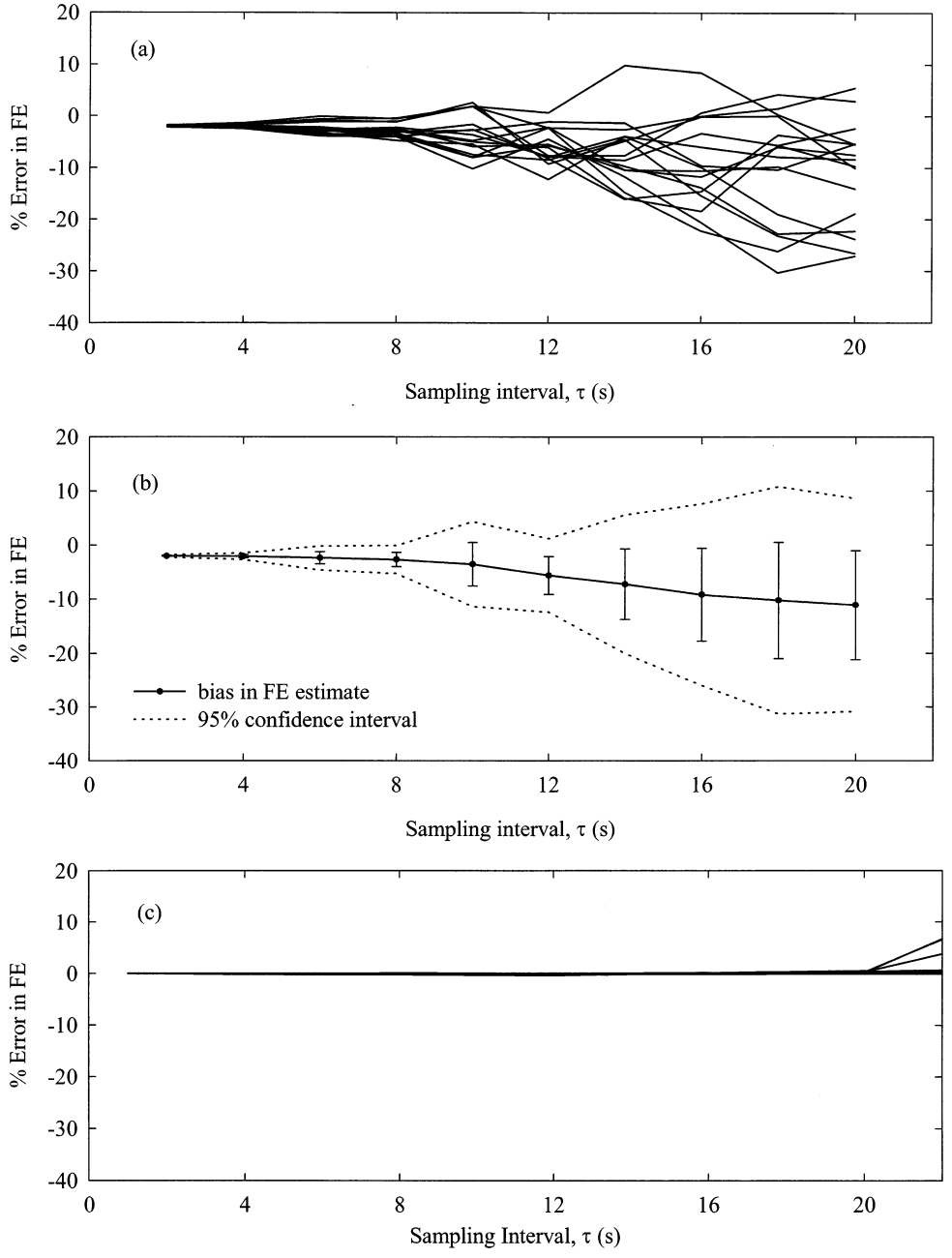

Fig. 5. (a) The relative error in the estimates of FE for 16 different combinations of δ/τ and ϵ/τ as a function of sampling interval, τ. Both the AIF and the TRF were sampled at the same rate. The true values for the kinetic parameters of the tissue were FE = 0.5 mL/min/g, V_e = 0.4 mL/g, and V_b = 0.05 mL/g. The AIF used corresponded to a 10-s bolus injection of contrast agent (1 × AIF). (b) Percentage bias in the mean of FE estimates plotted as a function of sampling interval. Error bars indicate the SD in the estimates caused by the temporal jitter effect, and the 95% confidence interval is also indicated. (c) The relative error in the estimates of FE for 16 different shifts of the TRF, ϵ/τ, if only the TRF is sampled, while the AIF is sampled every second. The same TRF and AIF as in (a) were used.

Effect of Tracer Kinetic Parameter Values

When both the AIF and TRF are sampled at the same rate, FE and V_e are underestimated while V_b tends to be overestimated (Fig. 9). The relative errors in the mean of all three parameters increase with increasing FE and decreasing V_e. The error in V_b is largest for small values of V_b, whereas the errors in FE and V_e are independent of the value of V_b. Uncertainties in the parameter esti-

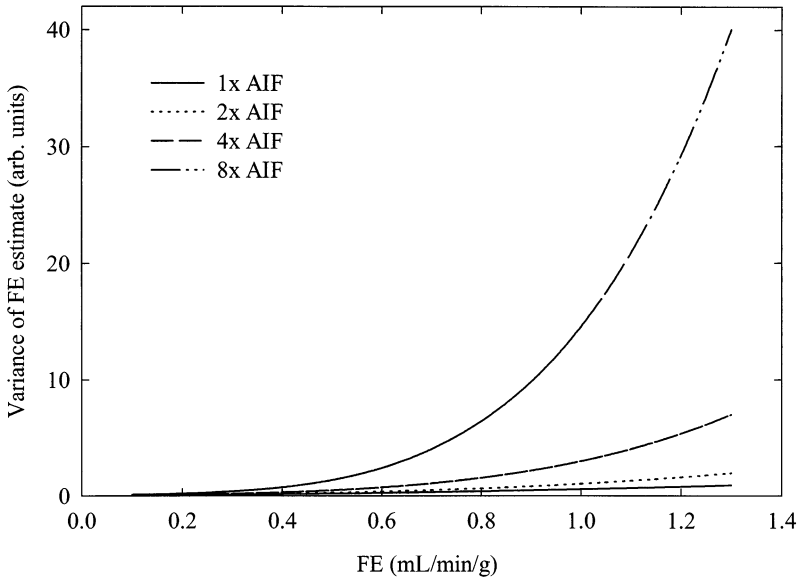

Fig. 6. Relative uncertainty in the FE estimate as predicted by COV matrix calculations plotted as a function of FE for several AIF widths.

mates (ΔB) follow the same general trends with parameter value as do the biases (B). Overall, the V_b parameter is by far the most sensitive to errors due to insufficient temporal sampling.

By sampling the AIF every second, the bias in all three parameters due to insufficient temporal sampling of the TRF can be reduced by approximately a factor of ten. For this sampling strategy, the trend is that all three parameters are underestimated (Fig. 10). In general, the relative errors in FE and V_e increase with increasing FE and decreasing V_e and are relatively independent of the value of V_b. The relative error in the V_b estimates has a more complex behaviour, but tends to increase with increasing FE and decreasing V_e and decrease with increasing V_b. Uncertainties in the parameter estimates follow the same general trends with parameter values. For very large sampling intervals ($\tau > 20$ s), however, B and ΔB become large due to the added effect of fit instability and trends with parameter values disappear, particularly for the narrowest AIF.

Maximum Allowable Sampling Interval

The results from the two sets of sampling simulations were compiled to determine what the maximum sampling interval, τ, would be to ensure, at a 95% confidence level, that the estimates of the tracer kinetic parameters are accurate to within 10% or 20%. As the width of the arterial input function is increased, the maximum allowable sampling interval decreases for both sampling strategies (Tables 2 and 3). If the AIF and TRF are sampled at the same rate, then for the original AIF ($1 \times$ AIF), which corresponds to a 10-s bolus injection of contrast agent, they must both be sampled in under 1 s for less than 10% error in all three parameters, or in under 2 s for less than 10% error in FE and V_e only (Table 2, Fig. 11). If, on the other hand, the AIF is sampled at 1-s intervals, then the temporal sampling constraints for the TRF can be relaxed significantly. For a 10-s bolus injection of contrast agent, the TRF must be sampled every 4 s to achieve less than 10% error in all three parameters, or every 16 s for less than 10% error in FE and V_e only (Table 3, Fig. 12). Recommendations for maximum τ are accurate to within 2 s for the sampling simulation in which the AIF and TRF are sampled at the same rate and to within 4 s for the sampling simulation in which only the TRF is sampled (and the AIF is sampled every second).

DISCUSSION

Tables 2 and 3 show that, for accurate measurements of FE, V_e, and V_b, the most important factor is that the AIF be finely sampled. If the AIF is sampled every second, then the TRF need only be sampled every 16 s for accurate (less than 10% error) estimates of FE and V_e or once every 4 s for accurate estimates of all three parameters. If a 20% error in the parameters can be tolerated, then the sampling requirements can be relaxed to once every 20 s for FE and V_e only, or once every 8 s for all three parameters. On the other hand, if the AIF and TRF are sampled at the same rate, then, at the 10% error limit, they must be sampled every 2 s for accurate esti-

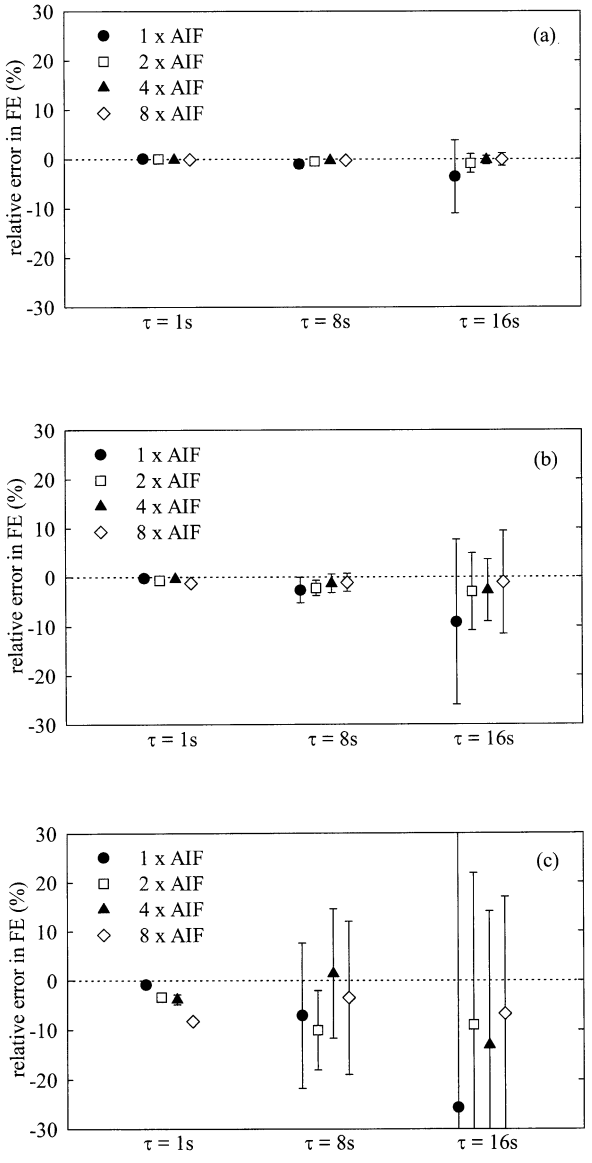

Fig. 7. Effect of sampling interval (τ) and width of the AIF on B and ΔB when the AIF and TRF are sampled at the same rate. Error bars represent the 95% confidence limits. V_e = 0.4 mL/g, V_b = 0.05 mL/g. (a) FE = 0.1 mL/min/g, (b) FE = 0.5 mL/min/g, (c) FE = 1.3 mL/min/g.

mates of FE and V_e only, or once every second for accurate estimates of all three parameters. Thus, although it may be most convenient to sample the AIF and the TRF simultaneously, there is a significant drawback to this strategy as both curves must be sampled at a very rapid rate. Conversely, if the AIF alone can be sampled sufficiently rapidly, then the temporal sampling requirements for the TRF can be relaxed significantly.

The plasma volume of breast tissue is small relative to FE, and therefore the tracer kinetics model is not very sensitive to the V_b parameter. The results of this study show that V_b is the parameter most affected by insufficient temporal sampling. For less than 10% error in V_b, the TRF must be sampled at least every 4 s if the AIF is sampled every second. Due to compromises made in order to attain a high spatial resolution or to image multiple slices or 3D volumes, this sampling rate will not be achieved in some studies, and therefore a significant error will be introduced into the V_b estimate. Nevertheless, the effect of contrast material in the vascular space should be included in the tracer kinetics model in order

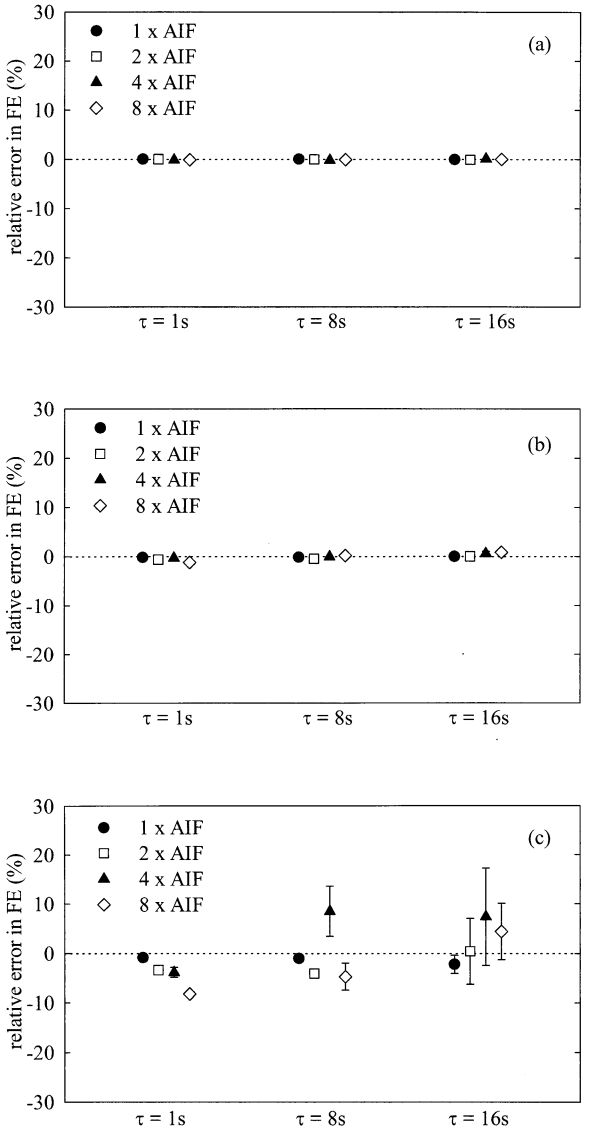

Fig. 8. Effect of sampling interval (τ) and width of the AIF on B and ΔB when only the TRF is sampled (and the AIF is sampled every second). Error bars represent the 95% confidence limits. V_e = 0.4 mL/g, V_b = 0.05 mL/g. (a) FE = 0.1 mL/min/g, (b) FE = 0.5 mL/min/g, (c) FE = 1.3 mL/min/g.

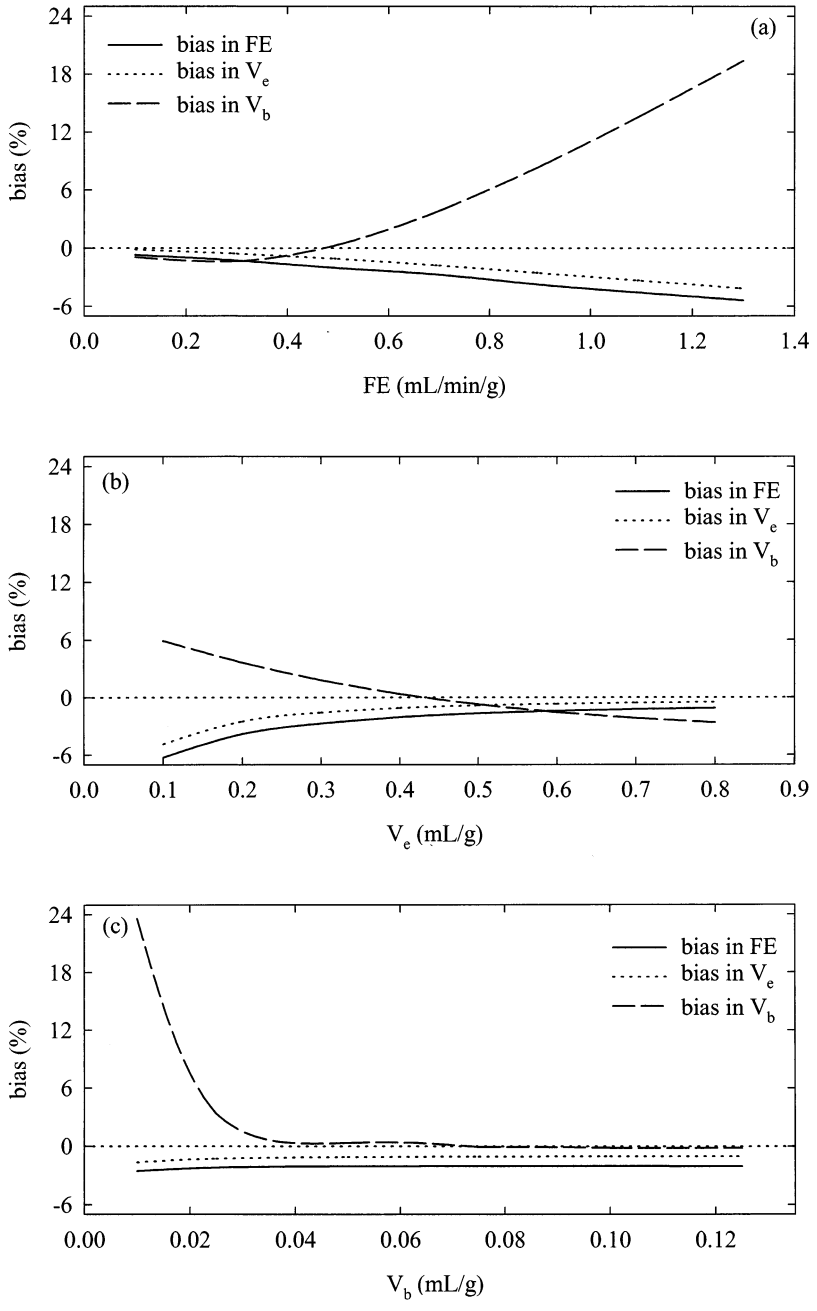

Fig. 9. Effect of parameter value on bias (B) if both the AIF and the TRF are sampled every 4 s, for a short bolus injection of contrast agent (1 × AIF). (a) Effect of varying FE, V_e = 0.4 mL/g, V_b = 0.05 mL/g. (b) Effect of varying V_e, FE = 0.5 mL/min/g, V_b = 0.05 mL/g. (c) Effect of varying V_b, FE = 0.5 mL/min/g, V_e = 0.4 mL/g.

to minimize error that would otherwise be introduced into estimates of the other two parameters.[42]

The results of the simulations, and examination of the model's sensitivity functions, show that there is no advantage to increasing the width of the AIF. In fact, for some values of the tracer kinetic parameters, there is a distinct disadvantage to using a wide AIF. As one might expect, the effect of broadening the AIF is to decrease the errors due to temporal under-sampling. This is seen as a decrease in ΔB for parameter sets that are relatively insensitive to sources of uncertainty—low values of FE, for example (Fig. 7a). We have seen, however, that temporal jitter, similar to noise in the TRF, introduces an uncertainty into the parameter estimates (Fig. 5). Be-

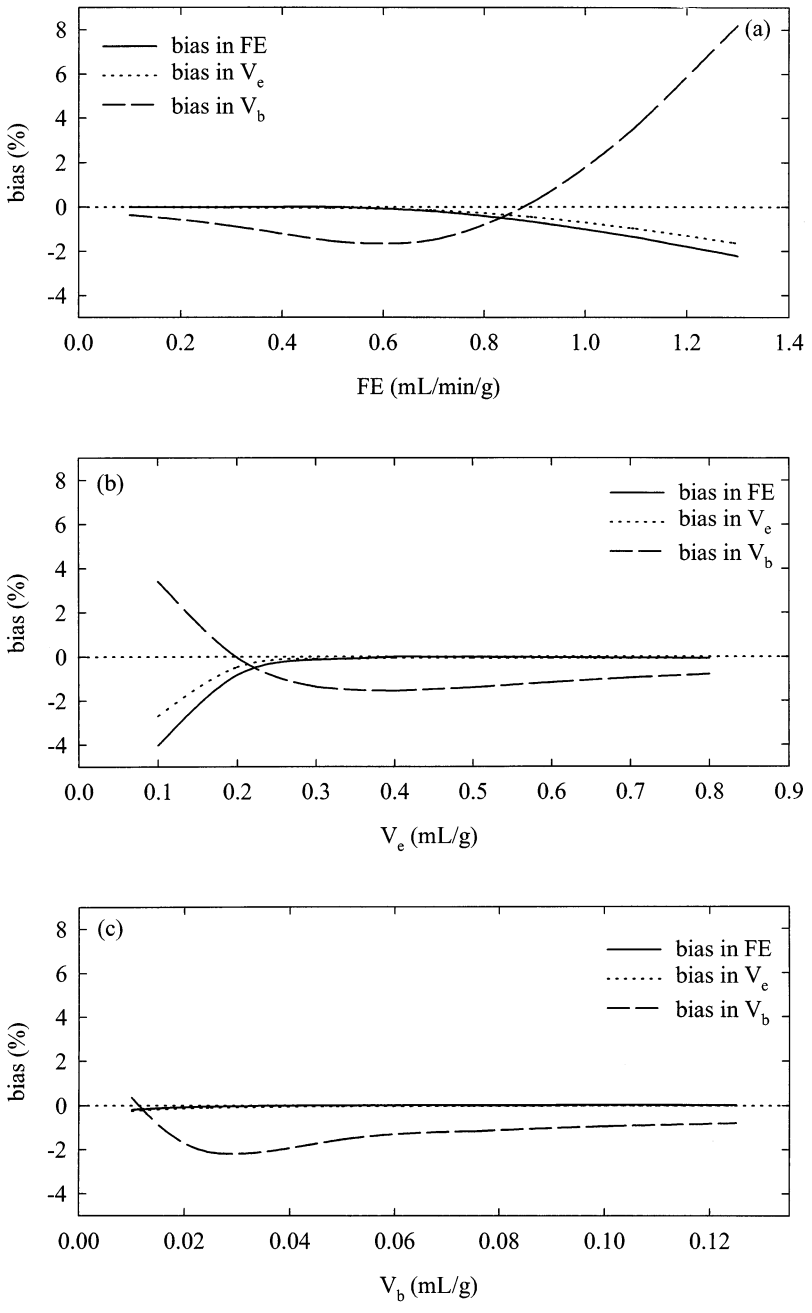

Fig. 10. Effect of parameter value on bias (B) if the TRF is sampled every 16 s and the AIF is sampled every second, for a short bolus injection of contrast agent (1 × AIF) (a) Effect of varying FE, V_e = 0.4 mL/g, V_b = 0.05 mL/g. (b) Effect of varying V_e, FE = 0.5 mL/min/g, V_b = 0.05 mL/g. (c) Effect of varying V_b, FE = 0.5 mL/min/g, V_e = 0.4 mL/g.

cause the COV matrices predict an increased sensitivity to noise with increased AIF width (Fig. 6), increasing the width of the AIF results in increased ΔB for some parameter values. Our simulations show that an increase in B is also seen in these cases. Tissues with high FE or low V_e or V_b are particularly vulnerable to this effect. For these parameter values, as predicted by the COV matrices, the model is hypersensitive to the uncertainties introduced by temporal jitter, and this effect dominates over any advantage gained by increasing the AIF width. Tables 2 and 3 show that the wider the AIF, the smaller the maximum sampling interval allowed for a certain allowable error in the parameters. Unfortunately, the value of FE in breast tumours can be high (Table 1), and

Table 2. Maximum τ recommendations for AIF and TRF sampled at same rate

	Maximum τ so that error in FE		Maximum τ so that error in V_e		Maximum τ so that error in V_b	
AIF	<10%	<20%	<10%	<20%	<10%	<20%
1 × AIF	2	4	4	6	1	1
2 × AIF	2	4	2	6	0	0
4 × AIF	2	4	2	6	0	0
8 × AIF	1	4	1	4	0	0

so in order to minimize errors due to the combined effects of temporal sampling and the inherent noise sensitivity of the model, the sharpest possible AIF should be used. In addition to this, it has been shown that a sharp bolus injection of contrast agent is more efficient at achieving tissue enhancement than is a longer constant infusion injection.[43] Based on these considerations, it seems clear that a rapid bolus injection of contrast agent is optimal for tracer kinetic studies of breast tissue.

Hoffman et al.[20] have also looked at the effects of temporal sampling of the TRF and of the width of the AIF on the accuracy and precision with which tracer kinetic parameters can be estimated in breast tissue. They examined the effect of temporal sampling of a TRF generated for one typical set of tissue parameters. In their case, they found that there is an advantage to using a wide AIF, and recommend that the TRF be sampled every 20 s. It is difficult to compare their results to ours, as they used a different tracer kinetics model. The model they used accounts for a long constant infusion of contrast agent and incorporates the shape of the AIF by modeling it as a monoexponential decay. Nevertheless, their results for the exchange parameter k_{21} ($\sim FE/V_e$)[31] are interesting with regards to our study. At the highest sampling rate (one sample every 20 s) studied, the bias in the mean of the k_{21} parameter estimates increased with AIF width while the uncertainty in the estimates stayed constant. At a low sampling rate (one sample every 80 s), B and ΔB decreased with increasing AIF width. We have observed similar trends, although over a higher range of sampling rates (Fig. 7). Kelcz et al.,[11] in a study in which they fit the enhancement profiles of breast tumours to the general saturation equation, also examined the effect of insufficient temporal sampling. The parameter that they measured, M, relates to the initial slope of the tissue enhancement curve. They found that the precision with which M can be estimated is a very strong function of temporal sampling rate, and that for a standard error of less than 20%, a temporal sampling rate of better than once every 4 s should be used.

Table 3. Maximum τ recommendations for TRF only (AIF sampled every second)

	Maximum τ so that error in FE		Maximum τ so that error in V_e		Maximum τ so that error in V_b	
AIF	<10%	<20%	<10%	<20%	<10%	<20%
1 × AIF	16*	20*	16*	20*	4	8
2 × AIF	8	16*	16*	16*	0	0
4 × AIF	4	4	4	24*	0	0
8 × AIF	1	8	4	24*	0	0

* Conservative estimate due to fit instability for $\tau \leq 20$ s.

Obviously, the results and recommendations of this study are only directly applicable to the tracer kinetics model we have examined (Eq. 1), as well as to the general form of the Tofts and Kermode model.[31,32] It is not certain how temporal sampling and temporal jitter would affect tracer kinetics studies in which other models are used, particularly since the effect of temporal sampling is so dependent on each model's sensitivity functions. The results of the two studies discussed above imply that some of the phenomena seen in this study do apply to studies in which other tracer kinetics models are used, although over a different range of temporal sampling rates. More extensive studies would be needed to verify this. The recommendations outlined in this paper can therefore only be used as a rough guide for studies in which tracer kinetics models other than that expressed by Eq. (1) are used.

We are not aware of any tracer kinetics modeling study of the breast in which a direct measurement of the AIF has been made. A common solution has been to use a general, well-defined AIF, whose shape represents an average over many healthy patients. This practice, however, introduces errors into the parameter estimates since, even if injection rate is controlled, there is considerable variability in cardiac output and renal clearance rate even among healthy volunteers. Although, according to our results, the sampling restrictions for the TRF could be reduced in this case, another error would be introduced by not knowing the exact AIF. Recently, however, there have been a number of efforts to develop methods for a non-invasive measurement of the AIF,[41,44–47] leading us to predict that it will soon be possible to measure both the AIF and TRF in the same study. The results of our simulations will be useful in determining the optimal design of these experiments. The result that the sampling constraints for the TRF can be relaxed considerably if the AIF is measured fast enough is particularly interesting. This implies that an interleaving strategy, such as that proposed by Taylor et al.[41] in which rapid imaging of a suitable artery is interleaved with slower two- or three-dimensional imaging of the breast tissue, has a large

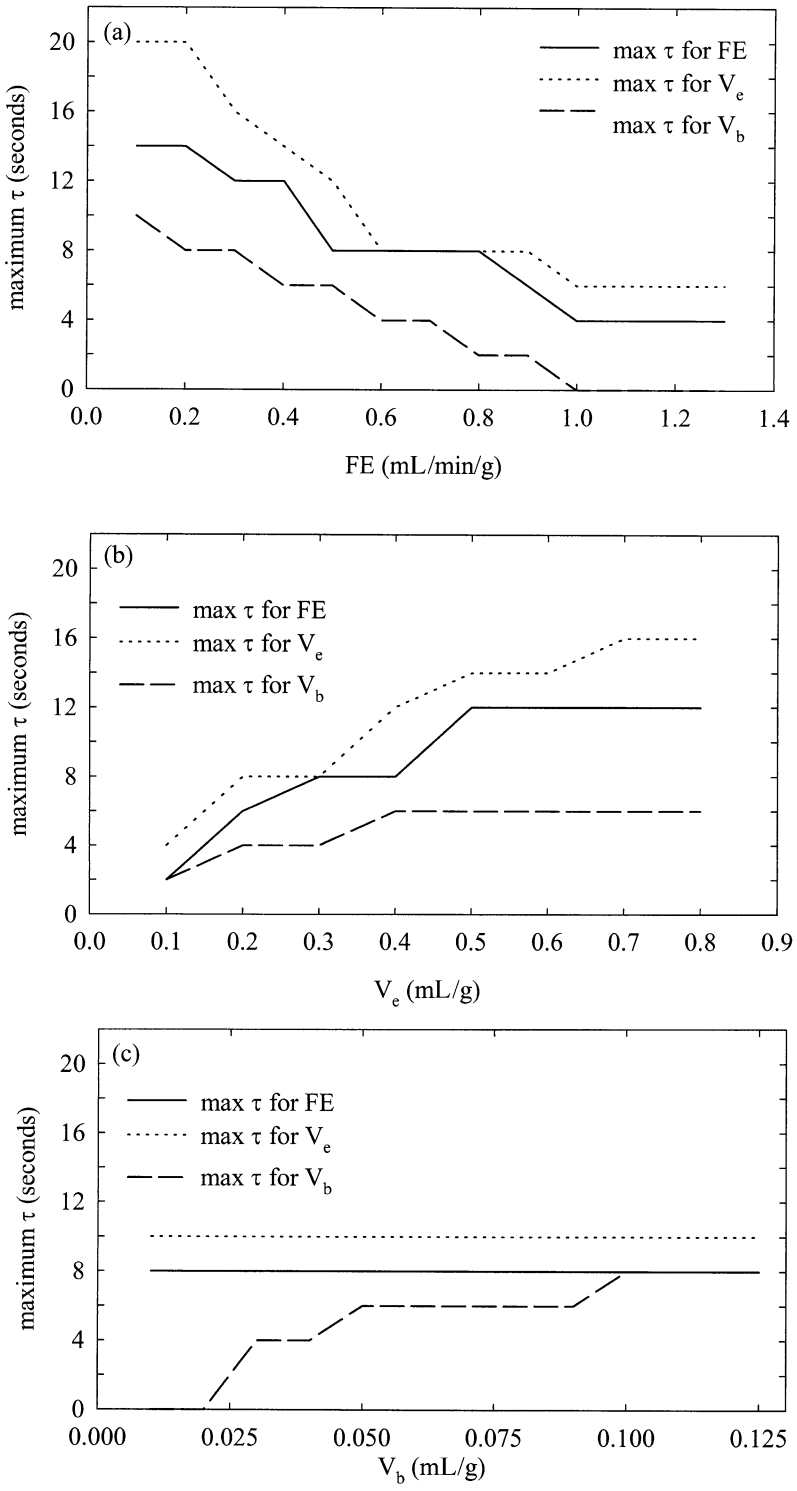

Fig. 11. Maximum τ requirement for the AIF and TRF as a function of (a) FE, (b) V_e, and (c) V_b if both the AIF and TRF are sampled at the same rate. A short bolus injection of contrast agent is assumed (1 × AIF).

advantage over strategies in which an artery, the aorta for example, is incorporated into the same field of view as the breast tissue and the AIF and TRF measured simultaneously. The high temporal resolution of the AIF enabled by the former strategy allows for improvements in the spatial resolution of the tissue images and opens up a

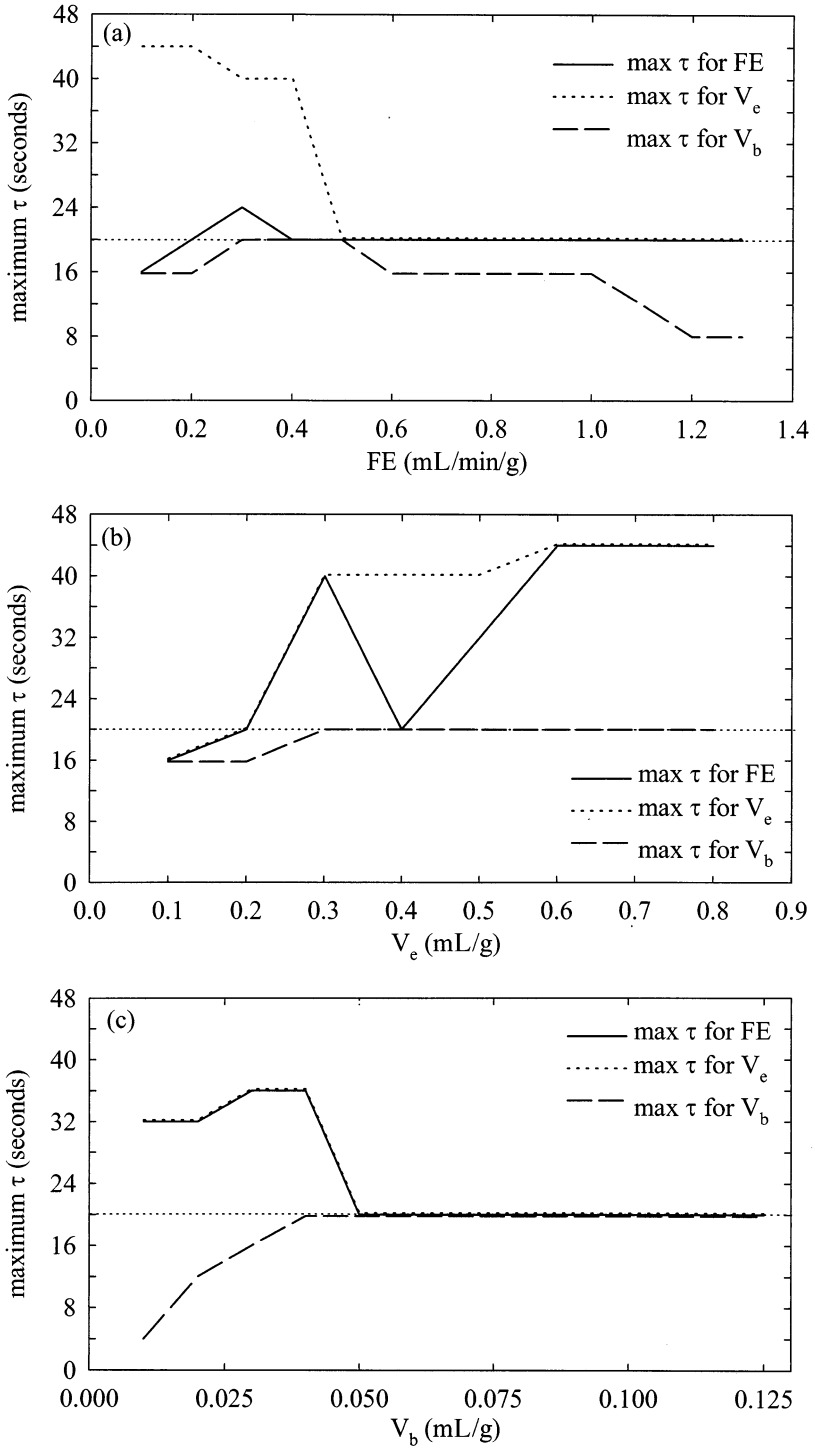

Fig. 12. Maximum τ requirement for the TRF as a function of (a) FE, (b) V_e, and (c) V_b if the AIF is sampled at 1-s intervals. A short bolus injection of contrast agent is assumed (1 × AIF). A horizontal line at $\tau = 20$ s indicates the sampling interval beyond which the fit becomes unstable. Because of the additional factor of fit instability for sampling intervals beyond t = 20 s, trends with parameter value are less clear than the trends shown in Fig. 11.

possibility for accurate tracer kinetics modeling of the data from dynamic 3D images.

In interpreting these results, one must keep in mind that not all possible sets of parameter values were investigated. In addition, the effect of noise, a major source of error in the measurement of tracer kinetics parameters,

was not considered. The recommendations for τ outlined in this paper should therefore be regarded as minimum recommendations. It is evident, however, that temporal sampling of the TRF in previous studies has often not been sufficient for accurate parameter estimates. Imaging times in various studies involving the tracer kinetics modeling of breast tissues have ranged between 6 and 30 s.[19,20,22–25] In many of these studies, temporal resolution was chosen to permit either higher spatial resolution, multiple slices, or 3D imaging. We have attempted to provide a better understanding of the errors introduced by insufficient temporal sampling of the arterial input function and tissue residue function in the tracer kinetics modeling of breast disease. The guidelines given will be useful in specifying temporal resolution and therefore the necessary trade-off in spatial resolution and other factors in future studies.

CONCLUSIONS

The results of our work have demonstrated the importance of injecting the contrast agent as rapidly as possible. For a rapid bolus injection, in order to achieve accurate estimates of FE and V_e (less than 10% error), either both the AIF and the TRF must be sampled every 4 s or less, or the AIF should be sampled very rapidly ($\sim$ every second) while the TRF should be sampled every 16 s or less. Finally, if an accurate estimate of V_b, in addition to FE and V_e, is to be made, then the TRF should be sampled every 4 s or less, with the AIF sampled at least every second.

Acknowledgment—This work was supported by the Canadian Breast Cancer Research Initiative, National Cancer Institute of Canada.

REFERENCES

1. Kaiser, W.A.; Zeitler, E. MR imaging of the breast: Fast imaging sequences with and without gadopentetate dimeglumine. Radiology 170:681–686; 1989.
2. Stack, J.P.; Redmond, O.M.; Codd, M.B.; Dervan, P.A.; Ennis, J.T. Breast disease tissue characterization with Gd-DTPA enhancement profiles. Radiology 174:491–494; 1990.
3. Hachiya, J.; Seki, T.; Okada, M.; Nitatori, T.; Korenaga, T.; Furuya, Y. MR imaging of the breast with gadopentetate dimeglumine enhancement: Comparison with mammography and ultrasonography. Radiat. Med. 9:232–240; 1991.
4. Gribbestad, I.S.; Nilsen, G.; Fjosne, H.E.; Kvinnsland, S.; Haugen, O.A.; Rinck, P.A. Comparative signal intensity measurements in dynamic gadolinium-enhanced MR mammography. J. Magn. Reson. Imaging 4:477–480; 1994.
5. Fobben, E.S.; Rubin C.Z.; Kalisher, L.; Dembner A.G.; Seltzer, M.H.; Santoro, E.J. Breast MR imaging with commercially available techniques: Radiologic-pathologic correlation. Radiology 196:143–152; 1995.
6. Turkat, T.J.; Klein, B.D.; Polan, R.L.; Richman, R.H. Dynamic MR mammography. A technique for potentially reducing the biopsy rate for benign breast disease. J. Magn. Reson. Imaging 4:563–568; 1994.
7. Boetes, C.; Barentsz, J.O.; Mus, R.D.; van der Sluis, R.F.; van Erning, L.J.T.O.; Hendriks, J.H.C.L.; Holland, R.; Ruys S.H.J. MR characterization of suspicious breast lesions with a gadolinium-enhanced turboFLASH subtraction technique. Radiology 193:777–781; 1994.
8. Stomper, P.C.; Herman, S.; Klippenstein, D.L.; Winston, J.S.; Edge, S.B.; Arredondo, M.A.; Mazurchuk, R.V.; Blumenson, L.E. Suspect breast lesions: Findings at dynamic gadolinium-enhanced MR imaging correlated with mammographic and pathologic features. Radiology 197:387–395; 1995.
9. Heiberg, E.V.; Perman, W.H.; Herrmann, V.M.; Janney, C.G. Dynamic sequential 3D gadolinium-enhanced MRI of the whole breast. Magn. Reson. Imaging 14:337–348; 1996.
10. Buadu, L.D.; Murakami, J.; Murayama, S.; Hashiguchi, N.; Sakai, S.; Masuda, K.; Toyoshima, S.; Kuroki, S.; Ohno, S. Breast lesions: Correlation of contrast medium enhancement patterns on MR images with histopathologic findings and tumor angiogenesis. Radiology 200:639–649; 1996.
11. Kelcz, F.; Santyr, G.E.; Cron, G.O.; Mongin, S.J. Application of a quantitative model to differentiate benign from malignant breast lesions detected by dynamic, gadolinium-enhanced MRI. J. Magn. Reson. Imaging 6:743–752; 1996.
12. Flickinger, F.W.; Allison, J.D.; Sherry, R.M.; Wright, J.C. Differentiation of benign from malignant breast masses by time-intensity evaluation of contrast enhanced MRI. Magn. Reson. Imaging 11:617–620; 1993.
13. Greenstein Orel, S.; Schnall, M.D.; LiVolsi, V.A., Troupin, R.H. Suspicious breast lesions: MR imaging with radiologic-pathologic correlation. Radiology 190:485–493; 1994.
14. Heywang-Kobrunner, S.H. Contrast-enhanced magnetic resonance imaging of the breast. Invest. Radiol. 29:94–104; 1994.
15. Folkman, J. Tumor angiogenesis: Therapeutic implications. N. Engl. J. Med. 285:1182–1186; 1971.
16. Folkman, J. What is the evidence that tumors are angiogenesis dependent? J. Natl. Cancer Inst. 82:4–6; 1990.
17. Weidner, N.; Semple, J.; Welch, W.R.; Folkman, J. Tumor angiogenesis and metastasis-correlation in invasive breast carcinoma. N. Engl. J. Med. 324:1–8; 1991.
18. Weidner, N.; Folkman, J.; Pozza, F.; Bevilacqua, P.; Allred, E.N.; Moore, D.H.; Meli, S.; Gasparini, G. Tumor angiogenesis: A new significant and independent prognostic indicator in early-stage breast carcinoma. J. Natl. Cancer Inst. 84:1875–1887; 1992.
19. Buckley, D.L.; Kerslake, R.W.; Blackband, S.J.; Horsman, A. Quantitative analysis of multi-slice Gd-DTPA enhanced dynamic MR images using an automated simplex minimization procedure. Magn, Reson, Med. 32:646–651; 1994.

20. Hoffman, U.; Brix, G.; Knopp, M.V.; Heβ, T.; Lorenz, W.J. Pharmacokinetic mapping of the breast: A new method for dynamic MR mammography. Magn. Reson. Med. 33:506–514; 1995.
21. Tofts, P.S.; Berkowitz, B.; Schnall, M.D. Quantitative analysis of dynamic Gd-DTPA enhancement in breast tumours using a permeability model. Magn. Reson. Med. 33:564–568; 1995.
22. Hulka, C.A.; Smith, B.L.; Sgroi, D.C.; Tan, L.; Edmister, W.B.; Semple, J.P.; Campbell, T.; Kopans, D.B.; Brady, T.J.; Weisskoff, R.M. Benign and malignant breast lesions: Differentiation with echo-planar MR imaging. Radiology 197:33–38; 1995.
23. Mussurakis, S.; Buckley, D.L.; Bowsley, S.J.; Carleton, P.J.; Fox, J.N.; Turnbull, L.W.; Horsman, A. Dynamic contrast-enhanced magnetic resonance imaging of the breast combined with pharmacokinetic analysis of gadolinium-DTPA uptake in the diagnosis of local recurrence of early-stage breast carcinoma. Invest. Radiol. 30:650–662; 1995.
24. den Boer, J.A.; Hoenderop, R.K.K.M.; Smink, J.; Dornseiffen, G.; Koch, P.W.A.A.; Mulder, J.H.; Slump, C.H.; Volker, E.D.P.; de Vos, R.A.I. Pharmacokinetic analysis of Gd-DTPA enhancement in dynamic three-dimensional MRI of breast lesions. J. Magn. Reson. Imaging 7:702–715; 1997.
25. Parker, G.J.M.; Suckling, J.; Tanner, S.F.; Padhani, A.R.; Revell, P.B.; Husband, J.E.; Leach, M.O. Probing tumor microvascularity by measurement, analysis, and display of contrast agent uptake kinetics. J. Magn. Reson. Imaging 7:564–574; 1997.
26. van Dijke, C.F.; Brasch, R.C.; Roberts, T.P.L.; Weidner, N.; Mathur, A.; Shames, D.M.; Mann, J.S.; Demsar, F.; Lang, P.; Schwickert, H.C. Mammary carcinoma model: Correlation of macromolecular contrast-enhanced MR imaging characterizations of tumor microvasculature and histologic capillary density. Radiology 198:813–818; 1996.
27. Parker, G.J.M.; Tanner, S.F.; Leach, M.O. Pitfalls in the measurement of tissue permeability over short time-scales using a low temporal resolution blood input function. In: Book of Abstracts: Fourth Annual Meeting of the International Society for Magnetic Resonance in Medicine, Vol. 3. Berkeley CA: ISMRM, 1996: p. 1582.
28. Henderson, E.; Lee, T.-Y.; Rutt, B.K. Tracer kinetics modeling of breast disease: Temporal sampling requirements. In: Book of Abstracts: Fifth Annual Meeting of the International Society for Magnetic Resonance in Medicine, Vol. 1. Berkeley CA: ISMRM, 1997: p. 145.
29. Lee, T.-Y.; Henderson, E. Improved tracer kinetics modeling for capillary permeability in tissues. In: Book of Abstracts: Fourth Annual Meeting of the International Society for Magnetic Resonance in Medicine, Vol. 2. Berkeley CA: ISMRM, 1996: p. 746.
30. St. Lawrence, K.; Lee, T.-Y. An adiabatic approximation to the tissue homogeneity model for water exchange in the brain: I. Theoretical derivation. J. Cereb. Blood Flow Metab., in press; 1998.
31. Tofts, P.S.; Kermode, A.G. Measurement of the blood-brain barrier permeability and leakage space using dynamic MR imaging. 1. Fundamental concepts. Magn. Reson. Med. 17:357–367; 1991.
32. Tofts, P.S. Modeling tracer kinetics in dynamic Gd-DTPA MR imaging. J. Magn. Reson. Imaging 7:91–101; 1997.
33. Larsson, H.B.W.; Stubgaard, M.; Frederiksen, J.L.; Jensen, M.; Henriksen, O.; Paulson, O.B. Quantitation of blood-brain barrier defect by magnetic resonance imaging and Gadolinium-DTPA in patients with Multiple Sclerosis and brain tumors. Magn. Reson. Med. 16:117–131; 1990.
34. Kenney, J.; Schmiedl, U.; Maravilla, K.; Starr, F.; Graham, M.; Spence, A.; Nelson, J. Measurement of blood-brain barrier permeability in a tumor model using magnetic resonance imaging with Gd-DTPA. Magn. Reson. Med. 27:68–75; 1992.
35. Tofts, P.S.; Berkowitz, B.A. Rapid measurement of capillary permeability using the early part of the dynamic Gd-DTPA MRI enhancement curve. J. Magn. Reson. Series B 102:129–136; 1993.
36. Huang, S.-C.; Phelps, M.E. Error in parameter estimates with variations in flow: measurement of oxygen utilization with positron-emission tomography. Circulation 72(Suppl. IV):77–80; 1985.
37. Seber, G.A.F.; Wild, C.J. Nonlinear regression. New York: John Wiley & Sons; 1989.
38. Andersen, C.; Taagehøj, J.F.; Mühler, A.; Rehling, M. Approximation of arterial input curve data in MRI estimation of cerebral blood-tumor-barrier leakage: Comparison between Gd-DTPA and $^{99\,m}$Tc-DTPA input curves. Magn. Reson. Imaging 14:235–241; 1996.
39. NAG Fortran Library - Mark 13, The Numerical Algorithms Group Limited, Downers Grove IL, 1988.
40. Brasch, R.; Pham, C.; Shames, D.; Roberts, T.; van Dijke, K.; van Bruggen, N.; Mann, J.; Ostrowitzki, S.; Melnyk, O. Assessing tumor angiogenesis using macromolecular MR imaging contrast media. J. Magn. Reson. Imaging 7:68–74; 1997.
41. Taylor, N.J.; Rowland, I.J.; Tanner, S.F.; Leach, M.O. A rapid interleaved method for measuring signal intensity curves in both blood and tissue during contrast agent administration. Magn. Reson. Med. 30:744–749; 1993.
42. Budinger, T.F.; Huesman, R.H. Ten precepts for quantitative data acquisition and analysis. Circulation 72(Suppl. IV):53–62; 1985.
43. Tofts, P.S.; Berkowitz, B.A. Measurement of capillary permeability from the Gd enhancement curve: A comparison of bolus and constant infusion injection methods. Magn. Reson. Imaging 12:81–91; 1994.
44. Fritz-Hansen, T.; Rostrup, E.; Larsson, H.B.W.; Søndergaard, L.; Ring, P.; Henriksen, O. Measurement of the arterial concentration of Gd-DPTA using MRI: A step toward quantitative perfusion imaging. Magn. Reson. Med. 36:225–231; 1996.
45. Akbudak, E.; Conturo, T.E. Arterial input functions from MR phase imaging. Magn. Reson. Med. 36:809–815; 1996.
46. Fischer, S.E.; Hofman, M.B.M.; Scott, M.; Wickline, S.A.;

Lorenz, C.H. Development and validation of a novel method for transforming input function signal intensity to [Gd-DTPA] for quantitative assessment of myocardial perfusion. In: Book of Abstracts: Fifth Annual Meeting of the International Society for Magnetic Resonance in Medicine, Vol. 2. Berkeley, CA: ISMRM, 1997: p. 848.

47. Edminster, W.B.; Schmidt, C.J.; Koelling, T.M.; Poncelet, B.P.; Kantor, H.L.; Weisskoff, R.M. Arterial Gd-DTPA concentration measurements with GE EPI and ΔR_2*. In: Book of Abstracts: Fifth Annual Meeting of the International Society for Magnetic Resonance in Medicine, Vol. 2. Berkeley, CA: ISMRM, 1997: p. 849.